


## Article

# Intervention of Artificial Neural Network with an Improved Activation Function to Predict the Performance and Emission Characteristics of a Biogas Powered Dual Fuel Engine

Vinay Arora <sup>1,\*</sup>, Sunil Kumar Mahla <sup>2,\*</sup>, Rohan Singh Leekha <sup>3</sup>, Amit Dhir <sup>4</sup>, Kyungroul Lee <sup>5,\*</sup> and Hoon Ko <sup>6</sup>

- <sup>1</sup> Computer Science & Engineering Department, Thapar Institute of Engineering and Technology, Patiala, Punjab 147004, India
- <sup>2</sup> Department of Mechanical Engineering, I.K. Gujral Punjab Technical University, Kapurthala 144603, India
- <sup>3</sup> Lead Application Support, IT-App Development/Maintenance, Concentrix, Gurugram 122001, India; leekharohan@gmail.com
- <sup>4</sup> Department of Energy & Environment, Thapar Institute of Engineering and Technology, Punjab 147004, India; amit.dhir@thapar.edu
- <sup>5</sup> School of Computer Software, Daegu Catholic University, Gyeongsan 38430, Korea
- <sup>6</sup> Information Technology Research Institute, Chosun University, Gwangju 61452, Korea; dr.hoonko@gmail.com
- \* Correspondence: vinay.arora@thapar.edu (V.A.); mahla.sunil@gmail.com (S.K.M.); carpedm@cu.ac.kr (K.L.)



**Citation:** Arora, V.; Mahla, S.K.; Leekha, R.S.; Dhir, A.; Lee, K.; Ko, H. Intervention of Artificial Neural Network with an Improved Activation Function to Predict the Performance and Emission Characteristics of a Biogas Powered Dual Fuel Engine. *Electronics* **2021**, *10*, 584. <https://doi.org/10.3390/electronics10050584>

Academic Editors: Nikolay Hinov and Valeri Mladenov

Received: 31 January 2021

Accepted: 17 February 2021

Published: 3 March 2021

**Publisher's Note:** MDPI stays neutral with regard to jurisdictional claims in published maps and institutional affiliations.



**Copyright:** © 2021 by the authors. Licensee MDPI, Basel, Switzerland. This article is an open access article distributed under the terms and conditions of the Creative Commons Attribution (CC BY) license (<https://creativecommons.org/licenses/by/4.0/>).

**Abstract:** Biogas is a significant renewable fuel derived by sources of biological origin. One of today's research issues is the effect of biofuels on engine efficiency. The experiments on the engine are complicated, time consuming and expensive. Furthermore, the evaluation cannot be carried out beyond the permissible limit. The purpose of this research is to build an artificial neural network successfully for dual fuel diesel engine with a view to overcoming experimental difficulties. Authors used engine load, bio-gas flow rate and n-butanol concentration as input parameters to forecast target variables in this analysis, i.e., smoke, brake thermal efficiency (BTE), carbon monoxide (CO), hydrocarbon (HC), nitrous-oxide (NO<sub>x</sub>). Estimated values and results of experiments were compared. The error analysis showed that the built model has quite accurately predicted the experimental results. This has been described by the value of Coefficient of determination (R<sup>2</sup>), which varies between 0.8493 and 0.9863 with the value of normalized mean square error (NMSE) between 0.0071 and 0.1182. The potency of the Nash-Sutcliffe coefficient of efficiency (NSCE) ranges from 0.821 to 0.8898 for BTE, HC, NO<sub>x</sub> and Smoke. This research has effectively emulated the on-board efficiency, emission, and combustion features of a dual-fuel biogas diesel engine taking the Swish activation mechanism in artificial neural network (ANN) model.

**Keywords:** bio-gas; dual fuel mode; artificial neural network; swish activation function; emission parameters; engine performance

## 1. Introduction

Due to higher fuel economy, greater performance and low fuel prices, diesel engines are now favoured in many industries. However, these engines' combustion emissions have long been negatively impacting civilization and habitat. Researchers are now emphasizing alternative fuels due to reduced fossil fuel supplies and concerns about the effect of the use of fossil fuels on ecological concerns, such as environmental pollution. To solve these challenges, diesel engine researchers plan to seek an appropriate, blended fuel that can improve the machine's efficiency and reduce emissions. Since traditional methods are very time-consuming and costly, researchers have turned to methods that could achieve the same performance more easily and efficiently. Artificial Neural Network (ANN) has already been used to develop computational technology for various automotive engineering problems [1].

ANNs have been used to handle a wide range of scientific and engineering challenges, especially in areas where traditional modelling approaches lack. An ANN's predictive capability benefits from experimental data training and then independent data validation. The off-line characterization of engine systems using machine learning models has a great prospective to create a very swift, scalable and versatile engine output and emissions model. ANN will assist in real time where there is no choice for tests by individual sensors or where the prospects of expense and practicality are overlooked. In addition, ANN modelling being fundamentally data-oriented is vulnerable to the intrinsic drawbacks related to overfitting, if posing operating data outside its training range. Therefore, the reliability of all such frameworks must be examined before implementation for real-time forecasts. ANN's flexibility in emulating the dynamics of performance and emission responses in a dual-fuel mode engine [2,3] has already been widely praised.

In order to approximate engine parameters, viz., pilot fuel flow rate, intake airflow rate and the exhaust gas temperature Naim Akkouche et al. [4] in 2020 built three models based on ANN. In their research findings the values for root mean square error (RMSE) ranged between 0.34 percent to 0.62 percent, while the  $R^2$  value ranges from 0.99 and 1. Kakatia et al. [5] used log-sigmoid to forecast the output for Soot, HC, CO<sub>2</sub>, NO<sub>x</sub>, CO and BSFCeq, taking inputs as oxygen, methanol flow rate, diesel flow rate, and air flow rate etc. Hariharana et al. [6] carried out experiments to assess the effects of using hydrogen (H<sub>2</sub>) and Lemon Grass Oil (LGO) as a selective diesel replacement fuel, in a Compression Ignition (CI) engine with single-cylinder. The ANN model has been developed using a regular backpropagation algorithm to predict the association between engine performance responses and input factors (i.e., load, LGO and hydrogen). To forecast brake specific fuel consumption (BSFC), overall in-cylinder pressure and exhaust emissions, Agbulut et al. [7] used ANN. For BSFC, NO<sub>x</sub>, CO, HC, and CPmax the  $R^2$  value obtained was 0.9995, 0.9999, 0.9902, 0.9990, and 0.9979 respectively.

Kurtgoz et al. [8] measured the thermal efficiency (TE), BSFC, and volumetric efficiency (VE) values of a spark ignition biogas engine taking varied ratios of engine loads and methane (CH<sub>4</sub>). To compare observed and expected values output metrics like correlation coefficient, mean absolute percentage error and root mean square error were used. Leo et al. [9] conducted an experimental study on a diesel/gasoline premixed HCCI-DI engine using WCO biodiesel as a direct injection fuel. Shojaeefard et al. [10] proposed a study in which the efficiency and emission characteristics of a castor oil biodiesel (COB)-diesel blended fuel in direct injection diesel engine were experimentally tested, and then forecast using ANN. Fuel mixes have been checked with varying biodiesel concentrations (0 percent, 5 percent, 10 percent, 15 percent, 20 percent, 25 percent, and 30 percent) at varying loads and speed of an engine. The feed-forward NN yielded  $R^2$  values of 0.999978–0.999998. Tests conducted by Shukri et al. [11], indicated that the blend of diesel fuel with palm oil and methyl ester have improved the engine efficiency. For the in-cylinder pressure, heat release, thermal efficiency, and volume, the  $R^2$  value of 0.996, 0.999, 0.989 and 0.998 was obtained respectively.

In order to assess the performance features of the variable compression ratio (VCR) CI engine Kumar et al. in [12] described the application of ANN. The performance parameters, viz., brake power, BTE, indicated power, indicated thermal efficiency, specific energy consumption, exergy efficiency, and exhaust gas temperature were taken for the research work. The model calculated the VCR diesel engine's output with regression coefficients between 0.996 and 0.997. Using two separate artificial intelligence approaches, i.e., ANN and support vector machines (SVM) for a four-stroke, four-cylinder diesel engine, vibration, noise level, and emission characteristics were investigated by Yildirim et al. in [13]. Hidayet et al. [14] applied ANN to the automotive sector as well as to several different areas of technology, and aimed for solving experimental problems by reducing expense, time and workforce waste. The output and exhaust temperature values of a gasoline engine were analyzed by Yusuf Cay in [15]. The fuel properties such as engine rpm, engine torque, mean effective pressure and injection timing were used at the input layer in order to train

the network; and the measurements of brake specific fuel consumption, effective power and engine exhaust temperature were anticipated. For training and testing datasets,  $R^2$  values of 0.99 were obtained; RMS values were lower than 0.02; and for test results, mean error percentage (MEP) values were lower than 2.7 percent. The sigmoid function was found to be the most commonly used activation function in models of the Artificial Neural Network in most of the studies so highlighted. The output varies from 0 to 1 for the sigmoid function, and from 0 to 0.25 for the derivatives of the sigmoid function. The Sigmoid is usually susceptible to the issue of vanishing gradient and method outcome is not zero-centered. In addition, the exponent and power operations make it costly to compute.

#### *Motivating Factor for This Research Work*

Intervention of data oriented artificial intelligence technologies has significant potential to build a really quick, responsive and reliable off-line engine system for predicting the engine efficiency and emission behavior within a selected simulation environment [16,17]. However, analyzing related experiments using the ANN approach to emulate pollution and output responses in a dual-fuel diesel context provides little or no consideration to the need to evoke relevant activation functions in order to rationalize the robustness of the proposed models. Thus, this research devises a meta-model to produce a trustworthy and steady virtual sensing framework for real-time prediction while characterizing emission and performance parameters in the biogas-diesel engine. Authors in this analysis have used engine load, bio-gas flow rate and concentration of n-butanol as input parameters to forecast target variables, viz., BTE, HC,  $\text{NO}_x$ , Smoke. The researchers used the swish activation function to build a three layered ANN model.

## 2. Materials and Methods

The low-in-sulphur diesel was procured from the Indian Oil Company Limited petrol station. In the current study, biogas was the essential fuel produced through anaerobic treatment of cow extracts and kitchen waste in a Deenbandhu-based facility of 6 m<sup>3</sup> capacity. Deenbandhu-based biogas plant has been traditionally used in provincial territories as cooking fuel. In a vault, the composite gas was stored and piped into the engine. To examine the physiochemical properties of fuels, the set standard of the American Society for Testing and Materials (ASTM) was used. Table 1 displays some associated fuel characteristics.

**Table 1.** Various traits of the test fuel along with its ASTM based test scheme (# Not provided by the supplier).

Features	Diesel	n-Butanol	Test Scheme (ASTM)	Biogas	Test Scheme (ASTM)
Density (kg/m <sup>3</sup> )@15 °C	840	810	D4052	0.92	D3588
Viscosity (mm <sup>2</sup> /s)@40 °C	2.72	3.64	D445		-
Heating Value (MJ/kg)	42.6	33.2	D4809	26.23	D1945
Flash Point (°C)	78	35	D93		
Fire Point (°C)	83	42	D93		
Cloud Point (°C)	−8	#	DL500		-
Pour Point (°C)	−6	−45	D97		
Cetane Number (CN)	50	22	D613		

Table 2 demonstrates the few additional properties of n-butanol fuel used to conduct the procedure with the biogas.

**Table 2.** Allied characteristics of the n-butanol [18,19].

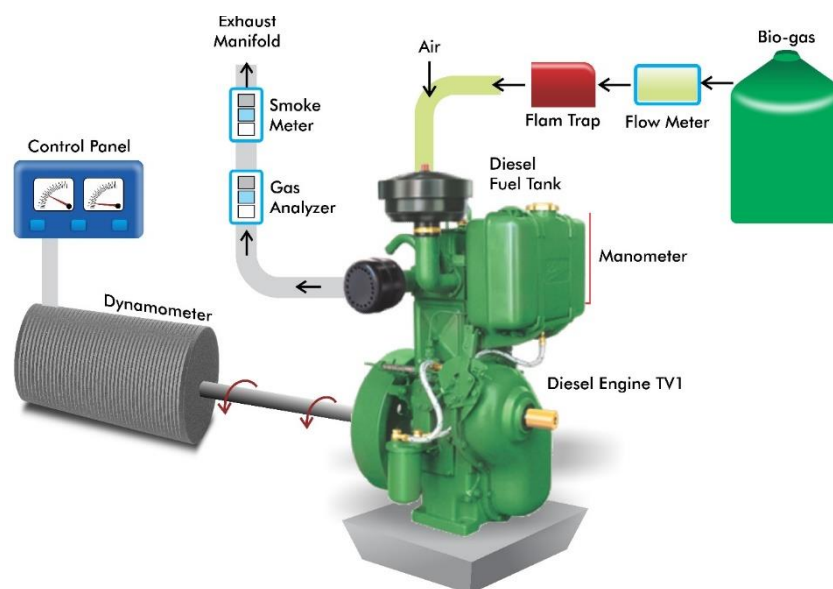
Chemical Formula	$C_4H_{10}O$
Boiling point	117 (°C)
Temperature for Auto ignition	343 (°C)
Octane number	96
Oxygen	21.62 (% by weight)
Latent heat of vaporization at 25 °C	626 (kJ/kg)

### Experimental Setup

The current research has used a four-stroke, direct-injection single-cylinder diesel engine with a 3.5 kW output at 1500 rpm. All tests were performed after the engine attained a steady 70 °C coolant temperature and a 1500 rpm speed. Table 3 lists test engine requirements. Figure 1 displays the configuration test summary.

**Table 3.** Feature set of the engine used here for conducting the experimentation.

Make	Kirloskar
Model Specifications	TV 1
System used for Cooling	Water Cooled
Cylinder Count	01
Rated Brake Power	5.2 kW @ 1500 rpm
Displacement volume	661 (cc)
Rated Speed	1500 (rpm)
Standard Fuel Injection Timing	23° before TDC
Bore × Stroke	87.5 × 110 (mm)
Compression Ratio	17.5:1

**Figure 1.** Diagrammatical depiction of the experimental setup used.

All fuel mixtures were checked at rated speed for engine efficiency and emission characteristics under different load conditions (20%, 40%, 60%, 80%, 100%). Biogas flow ranged at various speeds, i.e., 0.55, 1.55, 2.55 kg/h. N-butanol was volumetrically blended with baseline diesel at three proportions, i.e., nB10/D90, nB15/D95, and nB20/D80.

The CO, HC (unburned hydrocarbon), NO<sub>x</sub>, and Smoke were measured using a Di-gas analyser (AVL 4000). The % volume has been used to note CO and Smoke, whereas, gm/kW.hr for both HC and NO<sub>x</sub>. In order to measure smoke exhalation, a diesel smoke

metre (AVL 437) has been used; particularly the smoke opacity. In compliance with ASTM-D6522, the exhalations of gas are strictly regulated.

### 3. Application of Artificial Neural Network (ANN)

ANN is a computational model that is made up of an artificial neuron array. Mathematical equations determining the performance of a neural network are the activation functions. It is linked to every neuron in the network to decide whether or not it should be triggered (“fired”).

Every neuronal relation has a weight that reflects an ANN model’s memory. ANN can be used to treat strongly nonlinear, non-limiting and non-convex processes [20]. An ANN model’s performance depends on connection modes, weights, and activation functions that can be expressed as Equation (1):

$$y = f\left(\sum_j w_{ij}x_j + b\right) \quad (1)$$

$f \in \text{activation function}$   $w \in \text{weight}$   $x \in \text{input vector}$   $b \in \text{bias}$

#### 3.1. Back Propagation and ANN for Current Study

While methods have been employed to enhance ANN model predictive performance, back propagation (BP) neural network remains the most widely used techniques in this area. In back propagation, error values are propagated backward, whereas, the input vector is propagated forward. It usually has an input layer, a hidden layer, and a layer of output. In a standard BP neural network, Gradient descent algorithm has been used [18].

The aim of this analysis is to model the performance and emissions indices for a single cylinder diesel engine with dual fuel mode. Consequently, the ANN input vector provides essential parameters for evaluating the output and emission index. Model includes the input parameters as Bio-gas flow rate, engine load, and n-Butanol concentration. The outcome parameters were determined as BTE, CO, HC, NO<sub>x</sub> and Smoke. Figure 2 demonstrates the ANN model used here in this study work and Table 4 lists the parameter values used in ANN.

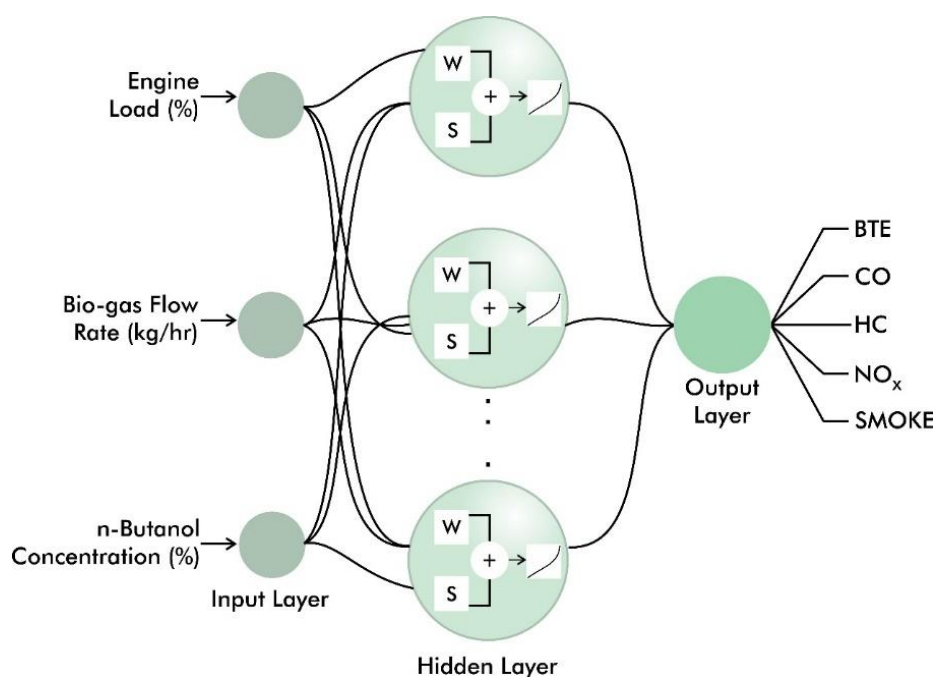


Figure 2. Structure of ANN model.



**Table 4.** Details related to the NN model used in this research.

Structure of the Network Used Here	3 inputs, 01 hidden layer, and 5 outputs
Percentage of Data used for training and testing	Training: 130 rows for training Testing: 20 rows for testing
Type of the Network	Feed Forward Back Propagation
Function used for Training	Backpropagation
Optimization Function	Adam
Transfer/Activation Function	<b>Swish</b>
Criteria used to Stop	On-set of enhancement in validation error will results into breaking of training network

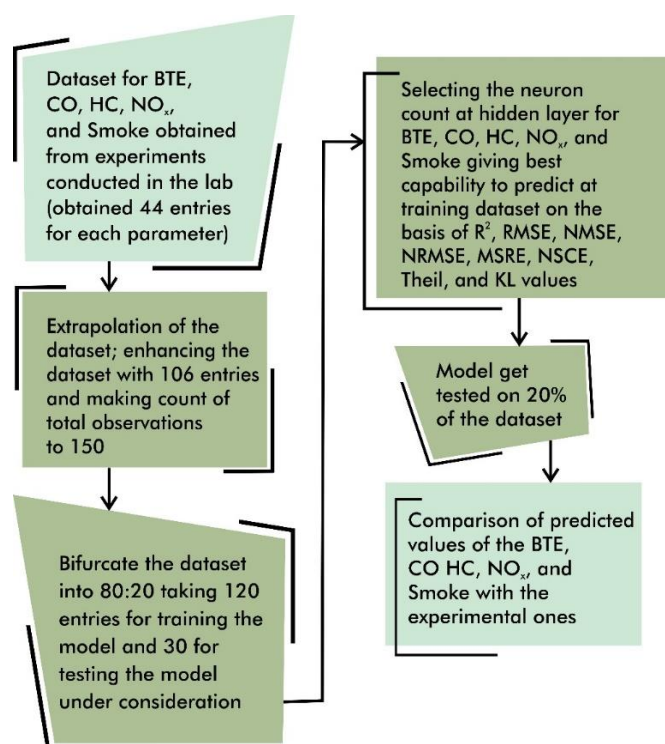
A single hidden layer network with only a small number of neurons can be trained to approximate a function with an arbitrary, but constrained, degree of randomness. In other words, in order to learn any feature, a single hidden layer is powerful enough. Growing the number of hidden layers adds to the issue of overfitting and vanishing gradients.

### 3.2. Swish Activation Function and Its Importance

Swish activation function zeroes the extreme negative weights. This offers advantages when tuning the convergence of the model to minimal loss. It is mathematically defined as [21]:

$$\text{swish}(x) = x \times \text{sigmoid}(\beta x) = \frac{x}{1 + e^{-\beta x}} \quad (2)$$

where,  $\beta$  is either a constant or trainable model parameter. For  $\beta = 1$ , the function is similar to the Sigmoid-weighted Linear Unit (SiL) function used in reinforcement learning. The functions are translated to the scaled linearly Equation  $f(x) = \frac{x}{2}$  for  $\beta = 0$ . In this research work, the steps that have been deployed for implementing ANN based model are depicted in Figure 3.

**Figure 3.** Steps followed for deploying ANN based model.

### 3.3. Count of Neurons for the Hidden Layer in ANN

One of ANN's big problems in modelling is preventing overfitting. When the network has been learned to predict its target performance with almost no error, it is often anticipated that the network can further forecast new data sets. Sometimes, however, new trends with higher error levels are expected due to data over fits. Selecting the required number of hidden nodes plays a vital role for bypassing data overfitting. Hecht-Nelson et al. [22] proposed a hidden neuron maximum bound using Kolmogorov's method as  $n_h \leq 2n_i + 1$ , where,  $n_i$  = count of input neurons,  $n_h$  = count of hidden neurons.

Considering Kolmogorov's formula the number of highest possible neurons at hidden layer is estimated as  $2 \times 3 + 1 = 7$ . Whereas, according to Belman-Flores et al. [23], the maximum neurons in single hidden layer can be computed using the formula  $n_T \geq c [n_h(n_i + 1)]$ , where,  $n_T$  = count of training sets.

With Belman-Flores equation, the maximum count of neurons in the hidden layer can be computed as:

$$n_h \leq \left\lceil \frac{n_T - cn_0}{c(n_i + n_0 + 1)} \right\rceil \quad (3)$$

where,  $c = 4$  is the coefficient value and count of outputs is referred as  $n_0$ . In this research work, neuron numbers can be determined as  $n_h \leq \left\lceil \frac{120 - 4 \times 5}{4(3 + 5 + 1)} \right\rceil = \frac{100}{36} = 2.77 \approx 3$ .

However, Belman-Flores et al. ( $n_h = 3$ ) and Hecht-Nelson et al. ( $n_h = 7$ ) estimated the lower neuron value as the maximum number of neurons in a single hidden layer structure [24]. The 3, 5 and 7 numbers of hidden neurons were therefore chosen for all of this analysis.

### 3.4. Selection among Sigmoid and Swish

Present literature indicates effectiveness of the sigmoid activation function in the ANN model for the field under study. Authors here used SWISH, an unexplored yet powerful activation function. For all said parameters, i.e., BTE, CO, HC, NO<sub>x</sub>, and Smoke, the value of RMSE was determined taking hidden neuron counts as 3, 5, and 7. ANN model employs sigmoid and swish activation function separately. Table 5 reveals that the RMSE values obtained for swish activation are lower relative to the commonly used sigmoid function, which proves swish, a better choice than the sigmoid. Also, when compared with rectified linear unit (ReLU) activation function, Swish is as effective as ReLU in computation, but demonstrates greater efficiency than ReLU. Swish values vary from infinity to infinity in the negative. The function curve is smooth and at all points the function is distinguishable, which is one of the reasons for outperforming swish from ReLU.

**Table 5.** RMSE value for BTE, CO, HC, NO<sub>x</sub>, and Smoke computed using swish and sigmoid activation function taking number of neurons as 3, 5 and 7 at hidden layer of the ANN model.

O/P	Transfer Function (At Layer 1-2-3)	No. of Neurons	RMSE
BTE	swish	3	1.741
		5	3.927
		7	3.288
	sigmoid	3	15.713
		5	15.693
		7	15.691

Table 5. Cont.

O/P	Transfer Function (At Layer 1-2-3)	No. of Neurons	RMSE
CO	swish	3	0.078
		5	0.059
		7	<b>0.056</b>
	sigmoid	3	0.08
		5	0.067
		7	0.078
HC	swish	3	<b>0.286</b>
		5	0.304
		7	0.307
	sigmoid	3	0.69
		5	0.61
		7	0.57
NO <sub>x</sub>	swish	3	1.491
		5	<b>1.435</b>
		7	2.207
	sigmoid	3	16.94
		5	16.863
		7	16.86
Smoke	swish	3	<b>2.448</b>
		5	3.154
		7	3.170
	sigmoid	3	20.327
		5	20.326
		7	20.31

#### 4. Model Evaluation

##### 4.1. Metrics for Evaluation

The authors evaluated the credibility of the established model in this analysis by confining it to the several error metrics and uncertainty estimation tests, which rationalised the validity of the proposed method. The Nash-Sutcliffe Coefficient of Efficiency (NSCE) Equation (4) correlation metric was used as a real model correlation assessment tool in order to prevent overestimated correlation as computed by standard  $R^2$  measure Equation (5), [25], which was found to be constrained by its intrinsic sensitivity to the expected and observed values of means and variances.

$$NSCE = \left[ 1 - \left\{ \frac{\sum_{i=1}^n (t_i - o_i)^2}{\sum_{i=1}^n (t_i - \bar{t})^2} \right\} \right] \quad (4)$$

$$R^2 = 1 - \left( \frac{\sum_{i=1}^n (t_i - o_i)^2}{\sum_{i=1}^n (o_i)^2} \right) \quad (5)$$

where,

$t_i$  = observed value

$o_i$  = predicted value

$n$  = count of elements under consideration



$\bar{t}$  = average of observed values

$\bar{o}$  = average of predicted values

In this research work, the root mean square error (RMSE) Equation (6) and normalized mean square error (NMSE) Equation (7) were used which are often recommended over mean square error (MSE), as MSE is much more prone to the outliers. Normalized value of RMSE, i.e., NRMSE, Equation (8) has been used, though, to reduce the scale dependence of RMSE, which allows a contrast across datasets of various size where lower value indicates smaller residual variance. In this analysis, mean square relative error (MSRE) Equation (9) was also used as an additional scale-independent metric indicator that determines the model's susceptibility to higher relative errors [2].

$$RMSE = \sqrt{\frac{1}{n} \sum_{i=1}^n (t_i - o_i)^2} \quad (6)$$

$$NMSE = \frac{1}{n} \sum_{i=1}^n \frac{(t_i - o_i)^2}{(\bar{t}) \times (\bar{o})} \quad (7)$$

$$NRMSE = \frac{\sqrt{\frac{1}{n} \sum_{i=1}^n (t_i - o_i)^2}}{t_{max} - t_{min}} \quad (8)$$

$$MSRE = \left| \frac{1}{n} \sum_{i=1}^n \left( \frac{t_i - o_i}{t_i} \right)^2 \right| \quad (9)$$

The Theil uncertainty metric, widely known as U2 suggested by Theil [26], is a predictive performance indicator of an established model. It gives a standardised calculation comparing the mean error of the predicted and observed values with the variance of errors. The lower value of the Theil implies greater model forecasting accuracy. In this current analysis [27], a KL-N metric model based on Kullback-Leibler (KL) divergence was used to determine the accuracy of the proposed ANN model. Lower divergence value indicates better generalisation potential of the model with better estimation efficiency index.

$$U2_{Theil} = \left[ \frac{\sqrt{\sum_{i=1}^n (t_i - o_i)^2}}{\sqrt{\sum_{i=1}^n t_i^2}} \right] \quad (10)$$

Centred on the Kullback-Leibler (KL) divergence, KL-N has been proposed, where, calculation corresponds to the scaled quadratic loss function with variance estimation. Its formula is:

$$KL = \sqrt{\frac{1}{n} \sum_{i=1}^n \frac{(t_i - o_i)^2}{S_{i,j}^2}} \quad (11)$$

where,  $S_{i,j}^2 = \frac{1}{j} \sum_{k=i-(j+1)}^{i-1} y_k$  and variance estimate has been used which considers the last  $j$  periods.

#### 4.2. Solver Architecture

In this work, an analytical method was used to pick optimal neurons in the hidden layer. As discussed in the Section 3.3, to stop overfitting, the maximum number of neurons was chosen as 3, 5 and 7. Table 6 provides  $R^2$ , RMSE, NMSE, NRMSE, MSRE, NSCE, Theil, and KL values computed at 3, 5, and 7 hidden layer neurons using ANN with SWISH activation function.

**Table 6.** Computation of  $R^2$ , RMSE, NMSE, NRMSE, MSRE, NSCE, Theil, KL using 3, 5, and 7 neurons at hidden layer with swish activation function while computing BTE, CO, HC,  $\text{NO}_x$ , and Smoke.

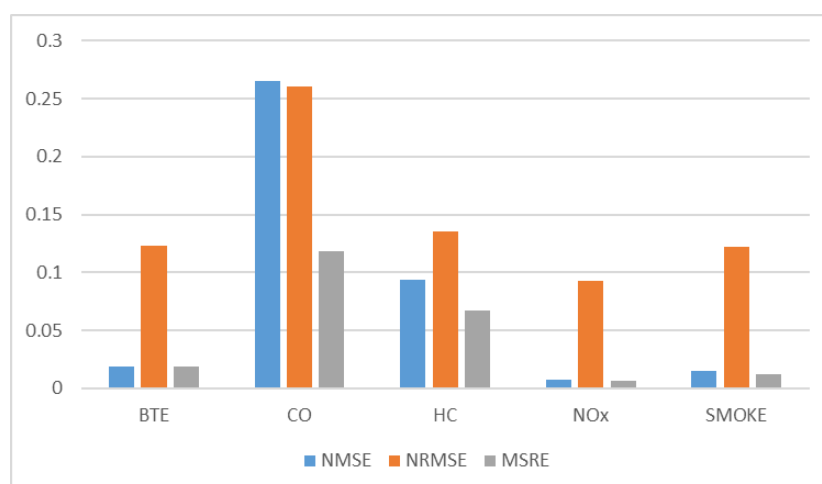
O/P	TF (At Layer 1-2-3)	No. of Neurons	R <sup>2</sup>	RMSE	NMSE	NRMSE	MSRE	NSCE	Theil	KL
BTE	swish + swish + swish	3	0.9705	1.741	0.0119	0.1235	0.0193	0.8211	0.1047	0.0068
		5	0.915	3.927	0.0716	0.2786	0.0405	0.0898	0.2361	0.008
		7	0.943	3.288	0.0489	0.2332	0.0282	0.3618	0.1977	0.007
CO		3	0.6576	0.078	0.2652	0.2609	0.1182	0.2497	0.3802	0.025
		5	0.8475	0.059	0.1332	0.199	0.0673	0.5635	0.29	0.018
		7	0.9332	0.056	0.1182	0.1872	0.0625	0.6139	0.2727	0.013
HC		3	0.9863	0.286	0.0938	0.1359	0.0673	0.8450	0.2294	0.016
		5	0.9038	0.304	0.1069	0.1441	0.0686	0.8256	0.2434	0.019
		7	0.9006	0.307	0.1101	0.1457	0.0629	0.8218	0.246	0.016
NO <sub>x</sub>		3	0.9923	1.491	0.0077	0.0932	0.0067	0.8810	0.0837	0.027
		5	0.9288	1.435	0.0071	0.0897	0.0064	0.8898	0.0805	0.028
		7	0.9813	2.207	0.0178	0.138	0.0129	0.7393	0.1239	0.04
Smoke		3	0.8493	2.448	0.0147	0.1224	0.0125	0.8209	0.1152	0.0079
		5	0.9817	3.154	0.0216	0.1577	0.028	0.7027	0.1484	0.0057
		7	0.9798	3.170	0.0299	0.1585	0.0211	0.6997	0.1491	0.0086

Table 6 and Figures 4–6 indicate that the model for 3 neurons has the potential to forecast BTE with significant precision, while for CO, 7 neurons are considerable. The optimal count of the neurons at hidden layer in the proposed ANN model to predict HC was found to be 3, while 5 and 3 neurons were found to predict  $\text{NO}_x$  and Smoke.

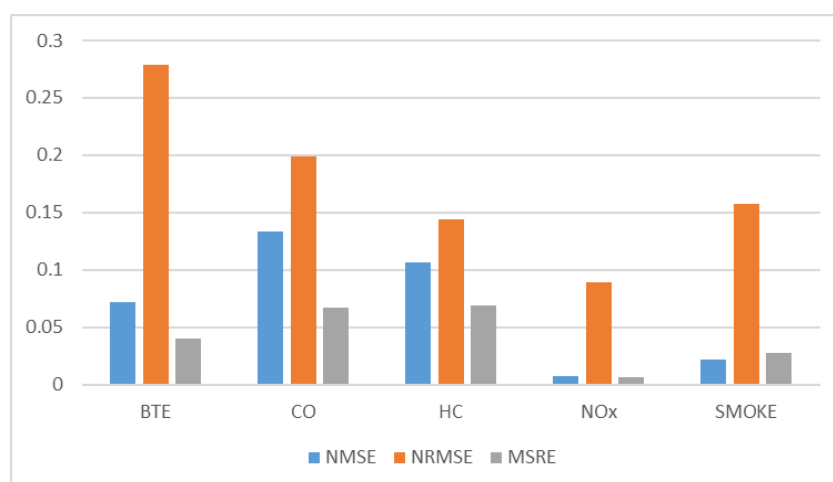
#### 4.3. Uncertainty Analysis for the Proposed Model

The ANN model was developed to forecast performance results such as BTE, CO, HC,  $\text{NO}_x$ , and Smoke; considering load, bio-gas flow rate, n-butanol as data, which was obtained from the experimental results. In this study, the model's predictability toward engine responsiveness showed good alignment with statistics of correlation. However, the complete uncertainty involved in measurement model derives from two distinct factors. One is the uncertainty of Theil that was considered in the development of the ANN model and the second is related to experimental tools. Total uncertainty estimation is seen in Table 7 using the Equation (12).

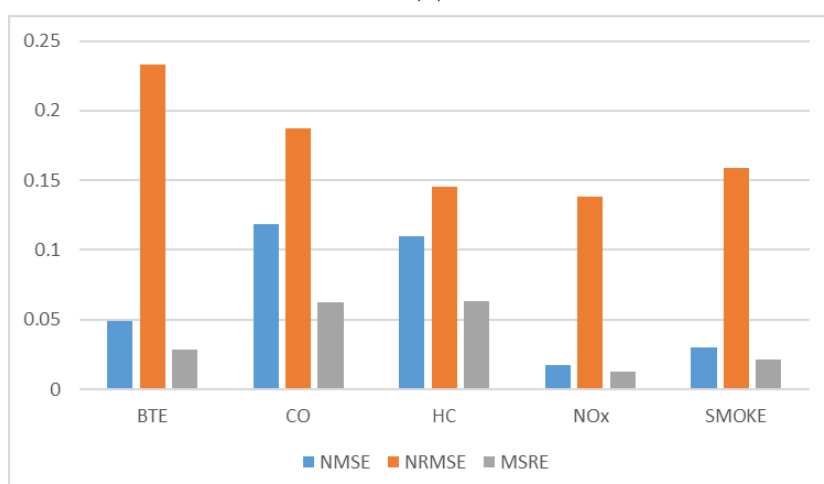
$$\text{Total Uncertainty} = \sqrt{(\text{Instrumental uncertainty})^2 + (\text{ANN Model Theil uncertainty})^2} \quad (12)$$



(a)

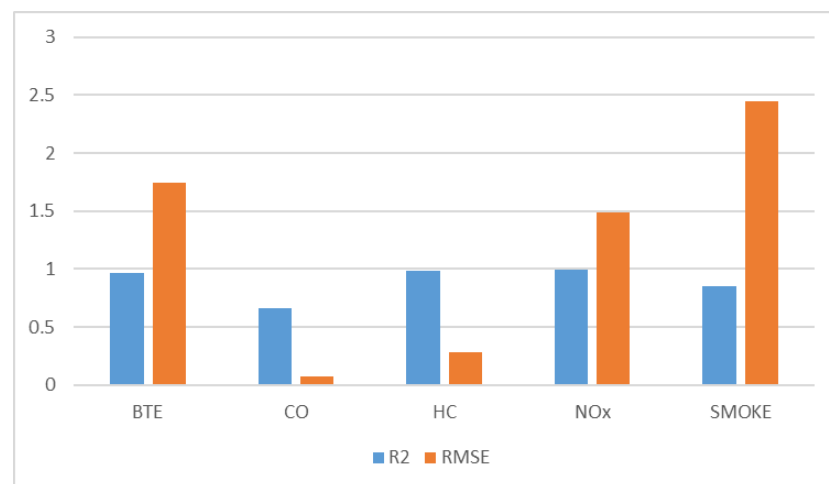


(b)

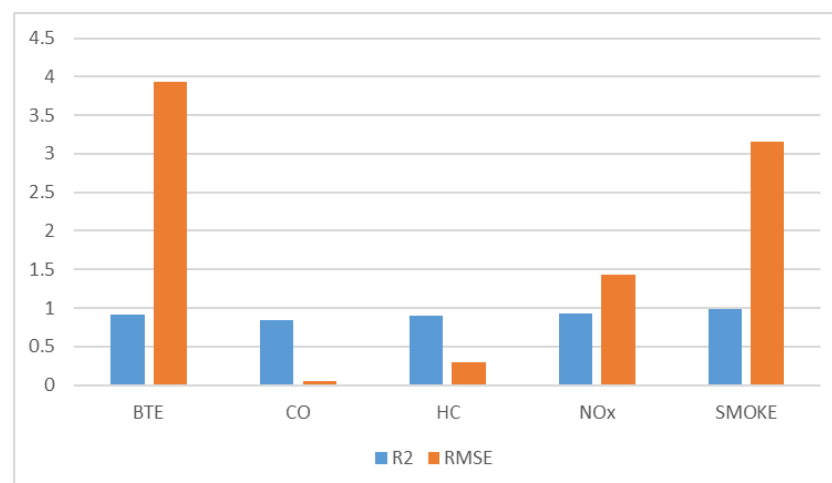


(c)

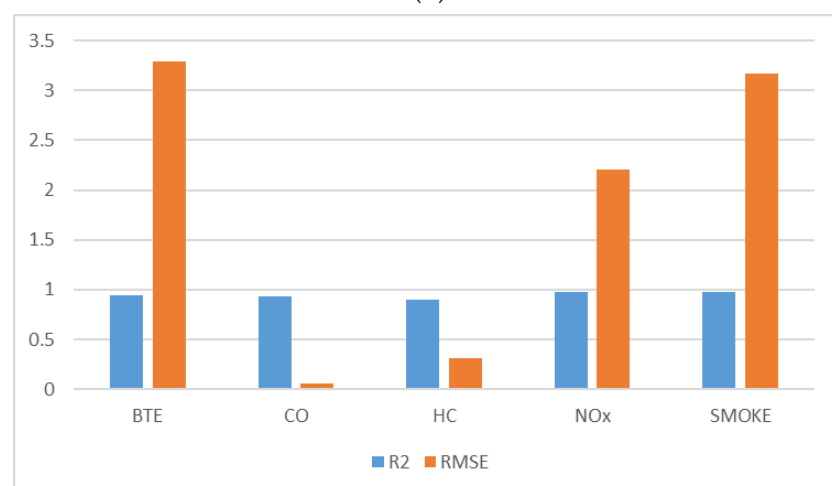
**Figure 4.** Depiction for comparing NMSE, NRMSE and MSRE of the model taking (a) 3 neurons; (b) 5 neurons; and (c) 7 neurons.



(a)

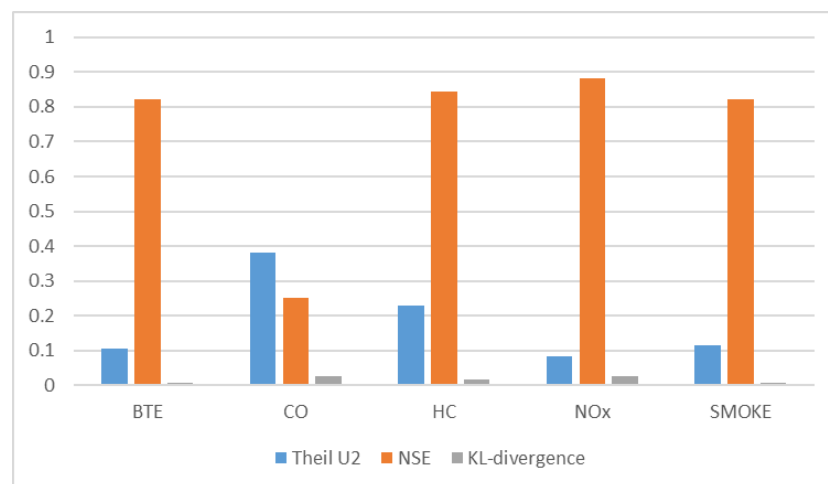


(b)

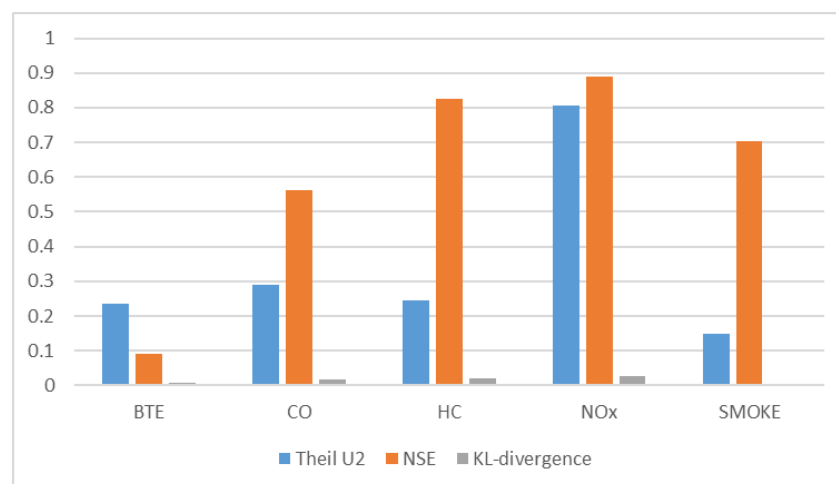


(c)

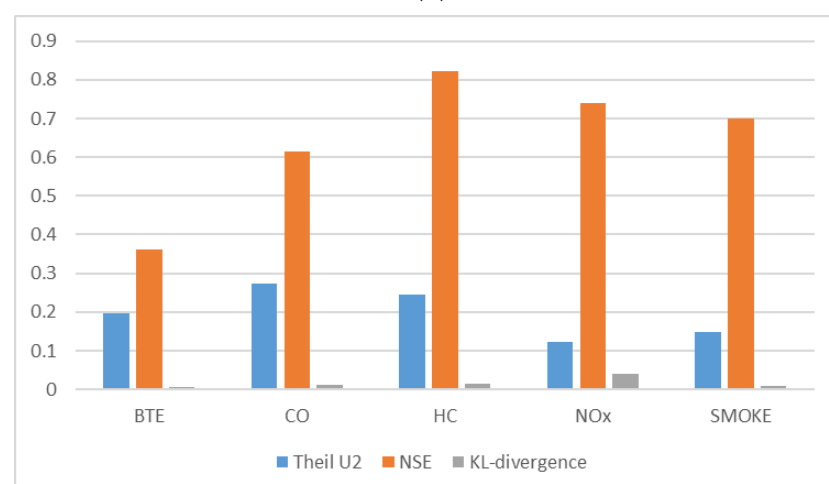
**Figure 5.** Illustration of  $R^2$  and RMSE of the model for (a) 3 neurons; (b) 5 neurons; and (c) 7 neurons.



(a)



(b)



(c)

**Figure 6.** Representation of values obtained with respect to Theil U2, NSE, and KL-divergence of the model for (a) 3 neurons, (b) 5 neurons, and (c) 7 neurons.

**Table 7.** Total uncertainty values obtained taking uncertainty values of the measuring instrument and the proposed ANN model.

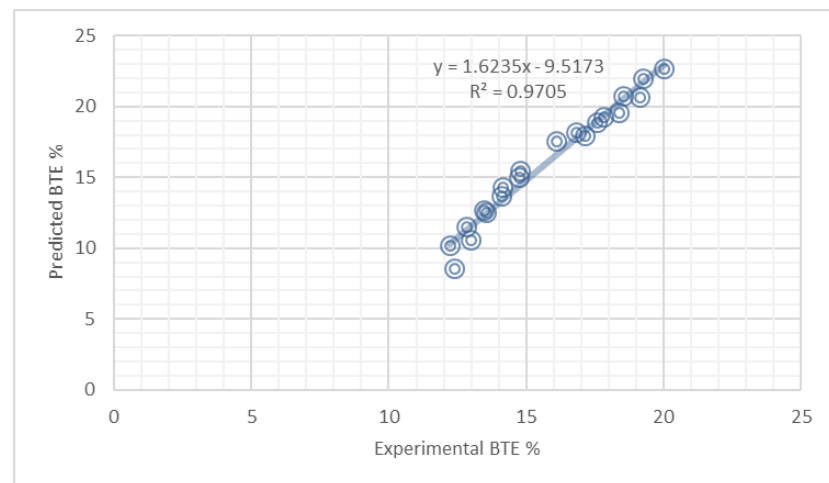
Parameters	Values for the Uncertainties	Computation	Cumulative Uncertainties $U_T$ (%)
BTE	2.5, 0.11	$\sqrt{(2.5)^2 + (0.11)^2}$	2.5024
CO	0.2, 0.27	$\sqrt{(0.2)^2 + (0.27)^2}$	0.3360
HC	0.1, 0.23	$\sqrt{(0.1)^2 + (0.23)^2}$	0.2507
NO <sub>x</sub>	0.2, 0.08	$\sqrt{(0.2)^2 + (0.08)^2}$	0.2154
Smoke	1, 0.11	$\sqrt{(1)^2 + (0.11)^2}$	1.0060

## 5. Results and Discussion

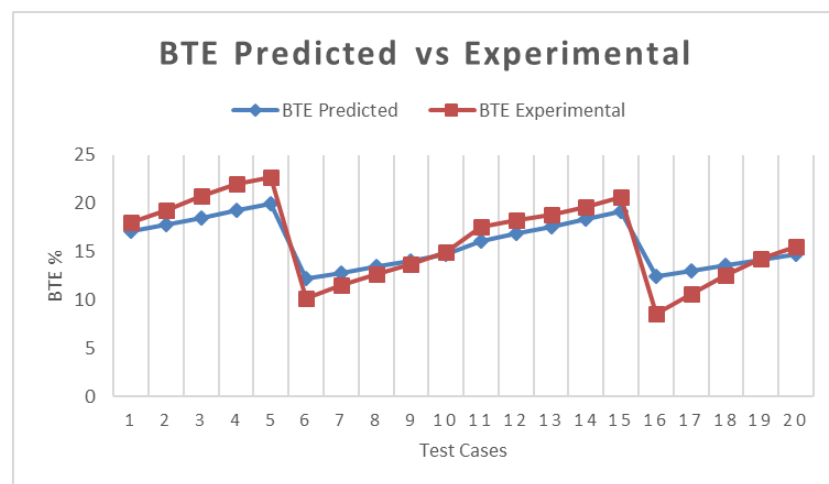
As seen in Figures 7–11, the expected values are laudably consistent with the real measurement for the entire engine operation. This indicates the forecast model's robustness to predict performance, emissions, and combustion specifications successively with excellent accuracy regardless of the engine's operation.

Figure 7 revealed the contrast of expected values vs. experimental BTE values. The predicted values display an exceptionally low 0.0193 MSRE with 0.1047 Theil uncertainty and 0.0068 KL-N prediction. NMSE and NRMSE were 0.0119 and 0.1235 for BTE. Nash-Sutcliffe Performance (NSCE) also demonstrated outstanding alignment with the experimental findings showing a value of 82.11%. Related trends were also noted for CO, as seen in Figure 8, in which the value of MSRE, NMSE, NRMSE was found to be 0.0625, 0.1182 and 0.1872. The Theil value was also found to be as minimal as 0.2727 along with KL-N as 0.013. For HC, Figure 9 indicates a very low MSRE and RMSE value of 0.0673 and 0.287 respectively. The value for the Theil uncertainty across all test points was found to be 0.2294. Figure 10 revealed statistical compatibility of predicted values with NO<sub>x</sub> experimental outcomes. It exhibits remarkably low 0.0805 Theil uncertainty along with 0.0064 MSRE. Other statistical tests such as NMSE, NRMSE also displayed very low significance, i.e., 0.0071 and 0.0897. NSCE was observed as high as 88.98 percent in special error metrics, while KL-N was reported to be 0.080 which fulfilled the stronger compatibility of expected values with experimental findings. Figure 11 showed the similarity of forecasted smoke by the model presented with observed smoke through experiments. The values for Smoke MSRE, NMSE and NRMSE were 0.0625, 0.1182 and 0.1872, respectively. With Theil's uncertainty as low as 0.1152, the model designed scored NSCE efficiency as high as 82.09 percent. In particular, a very low value of 0.0079 showed the KL-N divergence effectiveness, suggesting its good predictive accuracy.



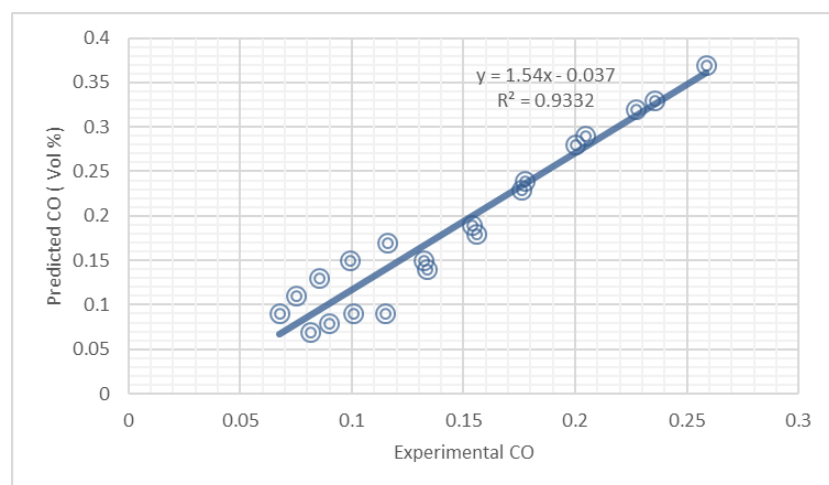


(a)



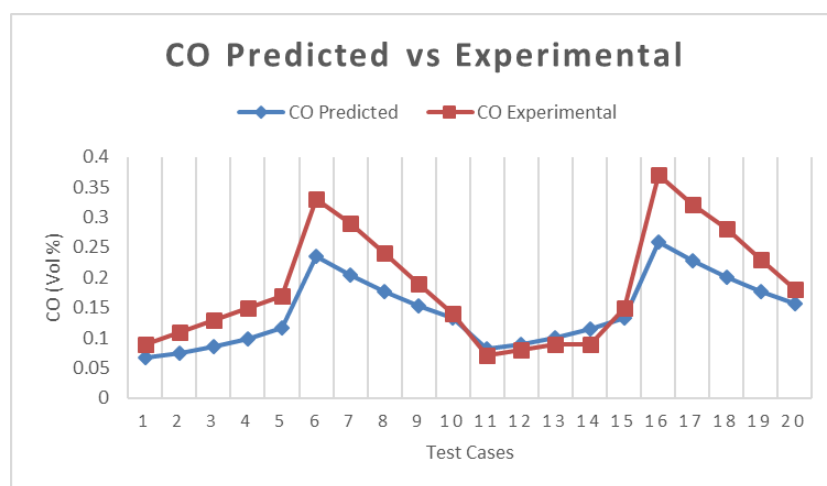
(b)

**Figure 7.** (a) Depiction of predicted and experimentally obtained BTE values taken for 20 test cases; (b) Regression coefficient for the values predicted using ANN Vs experimental.



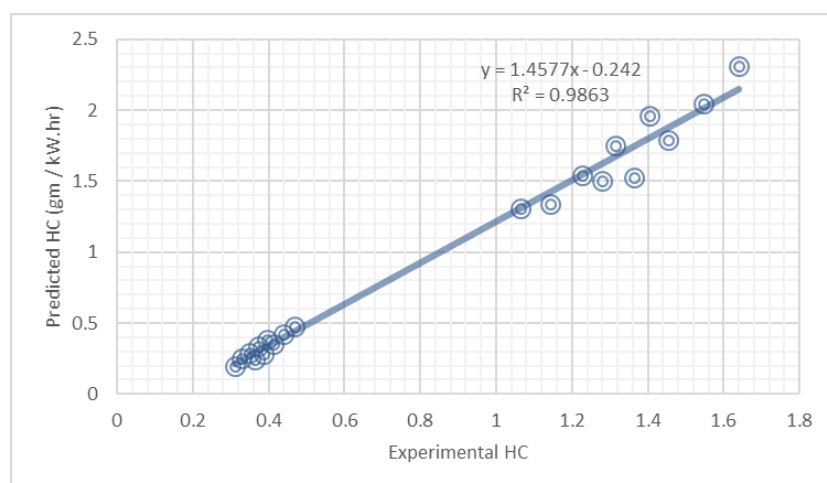
(a)

**Figure 8.** Cont.

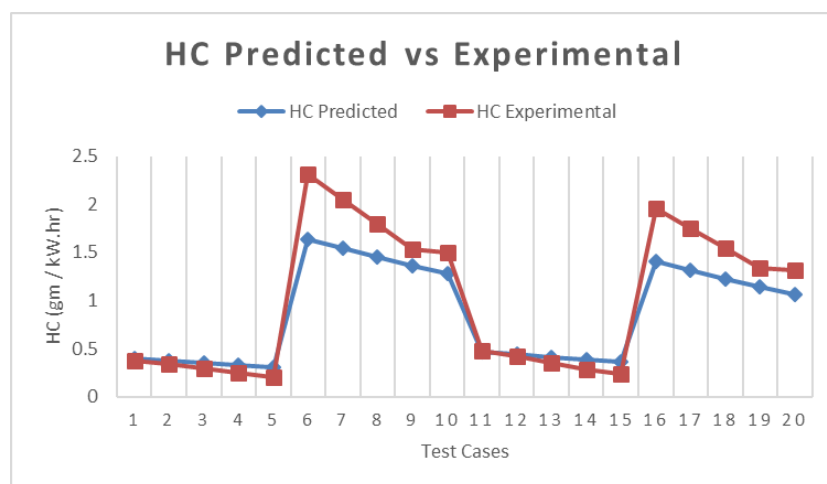


(b)

**Figure 8.** (a) Depiction of predicted and experimentally obtained CO values taken for 20 test cases; (b) Regression coefficient for the values predicted using ANN Vs experimental.

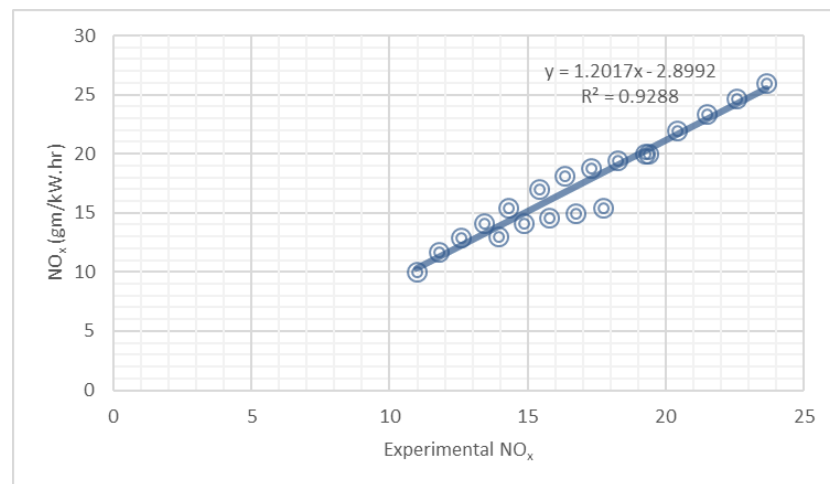


(a)

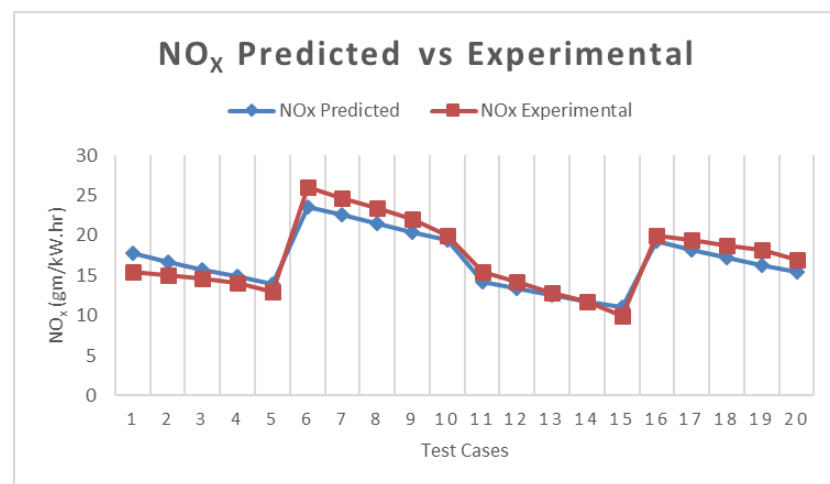


(b)

**Figure 9.** (a) Depiction of predicted and experimentally obtained HC values taken for 20 test cases; (b) Regression coefficient for the values predicted using ANN Vs experimental.

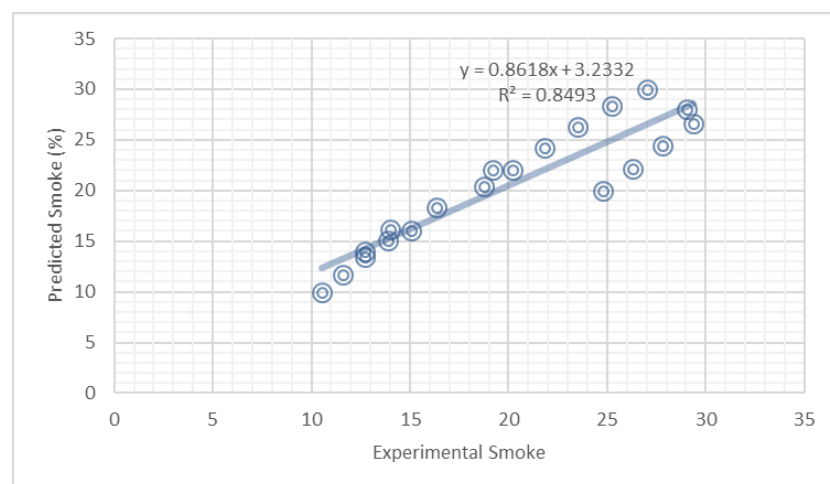


(a)



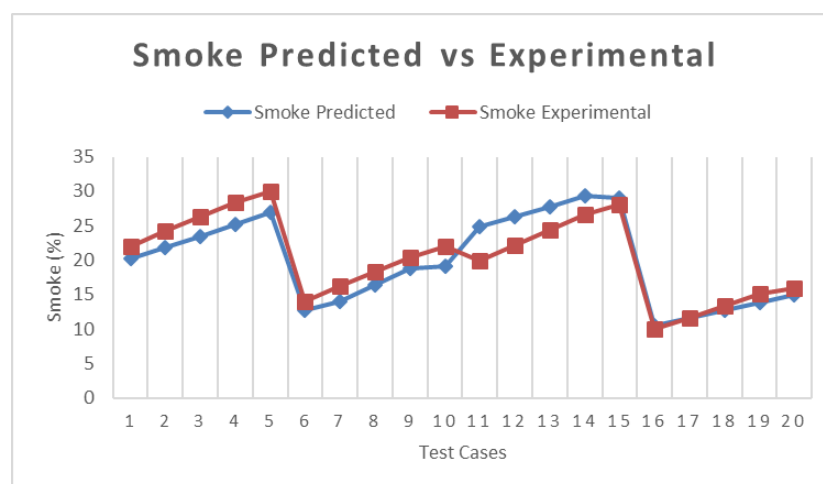
(b)

**Figure 10.** (a) Depiction of predicted and experimentally obtained  $\text{NO}_x$  values taken for 20 test cases; (b) Regression coefficient for the values predicted using ANN Vs experimental.



(a)

**Figure 11.** Cont.



(b)

**Figure 11.** (a) Depiction of predicted and experimentally obtained Smoke values taken for 20 test cases; (b) Regression coefficient for the values predicted using ANN Vs experimental.

## 6. Conclusions

In this analysis, a machine learning tool was used to forecast the efficiency, emissions and combustion variables of a dual-fuel biogas-diesel engine. Built ANN model includes a 3-neuron input layer, a single hidden layer of 3/5/7 neurons and a 5-neuron output layer. The error analysis showed that experimental outcomes were estimated with a robust degree of precision, with minimum  $R^2$  as 0.8493 and maximum as 0.9863. Also the values for NMSE spans between 0.0071 to 0.1182. NSCE performance ranged from 0.821 to 0.8898 for BTE, HC,  $\text{NO}_x$  and Smoke. The NSCE performance was found to range from 0.821 to 0.8898 for BTE, HC,  $\text{NO}_x$  and Smoke. Therefore, it can be concluded that the on-board performance and exhaust characteristics of a dual-fuel biogas-diesel engine can be effectively simulated by the proven ANN model.

**Author Contributions:** Conceptualization, V.A. and S.K.M.; methodology, V.A. and K.L.; software, R.S.L.; validation, R.S.L., H.K. and A.D.; formal analysis, K.L.; investigation, A.D.; resources, A.D.; data curation, A.D.; writing—original draft preparation, V.A.; writing—review and editing, V.A.; visualization, V.A. and R.S.L.; project administration, S.K.M. and V.A.; All authors have read and agreed to the published version of the manuscript.

**Funding:** This research was supported by Basic Science Research Program through the National Research Foundation of Korea (NRF) funded by the Ministry of Education (No. 2017R1A6A1A03015496).

**Acknowledgments:** This research was supported by Basic Science Research Program through the National Research Foundation of Korea (NRF) funded by the Ministry of Education (No. 2017R1A6A1A03015496). This research work is also supported by DST-SERB (India) sponsored R&D Project (Sanction No. SB/FTP/ETA-306/2013). This research was supported by the International Research & Development Program of the National Research Foundation of Korea (NRF) funded by the Ministry of Science and ICT (NRF-2020K1A3A1A79114935).

**Conflicts of Interest:** The authors declare no conflict of interest.

## References

- Roy, S.; Banerjee, R.; Bose, P.K. Performance and exhaust emissions prediction of a CRDI assisted single cylinder diesel engine coupled with EGR using artificial neural network. *Appl. Energy* **2014**, *119*, 330–340. [\[CrossRef\]](#)
- Banerjee, R.; Bose, P. Development of a neuro genetic algorithm based virtual sensing platform for the simultaneous prediction of  $\text{NO}_x$ , opacity and BSFC in a diesel engine operated in dual fuel mode with hydrogen under varying EGR conditions. *SAE Int. J. Engines* **2012**, *5*, 119–140. [\[CrossRef\]](#)
- Chakraborty, A.; Roy, S.; Banerjee, R. An experimental based ANN approach in mapping performance-emission characteristics of a diesel engine operating in dual-fuel mode with LPG. *J. Nat. Gas Sci. Eng.* **2016**, *28*, 15–30. [\[CrossRef\]](#)

4. Akkouche, N.; Loubar, K.; Nepveu, F.; Kadi, M.E.A.; Tazerout, M. Micro-combined heat and power using dual fuel engine and biogas from discontinuous anaerobic digestion. *Energy Convers. Manag.* **2020**, *205*, 112407. [\[CrossRef\]](#)
5. Kakati, D.; Roy, S.; Banerjee, R. Development of an artificial neural network based virtual sensing platform for the simultaneous prediction of emission-performance-stability parameters of a diesel engine operating in dual fuel mode with port injected methanol. *Energy Convers. Manag.* **2019**, *184*, 488–509. [\[CrossRef\]](#)
6. Hariharan, N.; Senthil, V.; Krishnamoorthi, M.; Karthic, S. Application of artificial neural network and response surface methodology for predicting and optimizing dual-fuel CI engine characteristics using hydrogen and bio fuel with water injection. *Fuel* **2020**, *270*, 117576. [\[CrossRef\]](#)
7. Ağbulut, Ü.; Ayyıldız, M.; Sarıdemir, S. Prediction of performance, combustion and emission characteristics for a dual fuel diesel engine at varying injection pressures. *Energy* **2020**, *197*, 117257. [\[CrossRef\]](#)
8. Kurtgoz, Y.; Karagoz, M.; Deniz, E. Biogas engine performance estimation using ANN. *Eng. Sci. Technol. Int. J.* **2017**, *20*, 1563–1570. [\[CrossRef\]](#)
9. Leo, G.L.; Sekar, S.; Arivazhagan, S. Experimental investigation and ANN modelling of the effects of diesel/gasoline premixing in a waste cooking oil-fuelled HCCI-DI engine. *J. Therm. Anal. Calorim.* **2020**, *141*, 2311–2324. [\[CrossRef\]](#)
10. Shojaeefard, M.; Etghani, M.; Akbari, M.; Khalkhali, A.; Ghobadian, B. Artificial neural networks based prediction of performance and exhaust emissions in direct injection engine using castor oil biodiesel-diesel blends. *J. Renew. Sustain. Energy* **2012**, *4*, 063130. [\[CrossRef\]](#)
11. Shukri, M.R.; Rahman, M.; Ramasamy, D.; Kadirgama, K. Artificial Neural Network Optimization Modeling on Engine Performance of Diesel Engine Using Biodiesel Fuel. *Int. J. Automot. Mech. Eng.* **2015**, *11*, 2332–2347. [\[CrossRef\]](#)
12. Ashok Kumar, T.; Musthafa, M.M.; Chandramouli, R.; Kandavel, T.; Mohanraj, T.; Sridharan, G. Performance characteristics of a variable compression ratio CI engine simulation using artificial neural network. *Energy Sources Part A Recover. Util. Environ. Eff.* **2019**, *23*, 1–11. [\[CrossRef\]](#)
13. Yıldırım, S.; Tosun, E.; Çalık, A.; Uluocak, İ.; Avşar, E. Artificial intelligence techniques for the vibration, noise, and emission characteristics of a hydrogen-enriched diesel engine. *Energy Sources Part A Recover. Util. Environ. Eff.* **2019**, *41*, 2194–2206. [\[CrossRef\]](#)
14. Oğuz, H.; Sarıtas, I.; Baydan, H.E. Prediction of diesel engine performance using biofuels with artificial neural network. *Expert Syst. Appl.* **2010**, *37*, 6579–6586. [\[CrossRef\]](#)
15. Cay, Y. Prediction of a gasoline engine performance with artificial neural network. *Fuel* **2013**, *111*, 324–331. [\[CrossRef\]](#)
16. Shayler, P.; Goodman, M.; Ma, T. The exploitation of neural networks in automotive engine management systems. *Eng. Appl. Artif. Intell.* **2000**, *13*, 147–157. [\[CrossRef\]](#)
17. Papadimitriou, I.; Warner, M.; Silvestri, J.; Lennblad, J.; Tabar, S. Neural network based fast-running engine models for control-oriented applications. *SAE Tech. Pap.* **2005**, *13*, 214–233.
18. Mahla, S.K.; Ardebili, S.M.S.; Sharma, H.; Dhir, A.; Goga, G.; Solmaz, H. Determination and utilization of optimal diesel/n-butanol/biogas derivation for small utility dual fuel diesel engine. *Fuel* **2021**, *289*, 119913. [\[CrossRef\]](#)
19. Imtenan, S.; Masjuki, H.H.; Varman, M.; Fattah, I.M.R. Evaluation of n-butanol as an oxygenated additive to improve combustion-emission-performance characteristics of a diesel engine fuelled with a diesel-calophyllum inophyllum biodiesel blend. *RSC Adv.* **2015**, *5*, 17160–17170. [\[CrossRef\]](#)
20. Yang, F.; Cho, H.; Zhang, H.; Zhang, J.; Wu, Y. Artificial neural network (ANN) based prediction and optimization of an organic Rankine cycle (ORC) for diesel engine waste heat recovery. *Energy Convers. Manag.* **2018**, *164*, 15–26. [\[CrossRef\]](#)
21. Celebi, M.; Ceylan, M. The New Activation Function for Complex Valued Neural Networks: Complex Swish Function. In Proceedings of the 4th International Symposium on Innovative Approaches in Engineering and Natural Sciences, Samsun, Turkey, 22–24 November 2019.
22. Hecht-Nielsen, R. Kolmogorov's mapping neural network existence theorem. Proceedings of the international conference on Neural Networks. *IEEE Press N. Y.* **1987**, *3*, 11–14.
23. Belman-Flores, J.M.; Ledesma, S.; Garcia, M.; Ruiz, J.; Rodríguez-Muñoz, J.L. Analysis of a variable speed vapor compression system using artificial neural networks. *Expert Syst. Appl.* **2013**, *40*, 4362–4369. [\[CrossRef\]](#)
24. Gandomi, A.H.; Roke, D.A. Assessment of artificial neural network and genetic programming as predictive tools. *Adv. Eng. Softw.* **2015**, *88*, 63–72. [\[CrossRef\]](#)
25. Yassin, M.A.; Alazba, A.; Mattar, M.A. Artificial neural networks versus gene expression programming for estimating reference evapotranspiration in arid climate. *Agric. Water Manag.* **2016**, *163*, 110–124. [\[CrossRef\]](#)
26. Kshirsagar, C.M.; Anand, R. Artificial neural network applied forecast on a parametric study of Calophyllum inophyllum methyl ester-diesel engine out responses. *Appl. Energy* **2017**, *189*, 555–567. [\[CrossRef\]](#)
27. Chen, Z.; Yang, Y. *Assessing Forecast Accuracy Measures*; Technical Report 2004–10; Iowa State University, Department of Statistics & Statistical Laboratory: Ames, IA, USA, 2004.